

# Time-reversal solution of BSDEs in stochastic optimal control: a linear quadratic study

Yuhang Mei<sup>1</sup> and Amirhossein Taghvaei<sup>1</sup>

**Abstract**—This paper addresses the numerical solution of backward stochastic differential equations (BSDEs) arising in stochastic optimal control. Specifically, we investigate two BSDEs: one derived from the Hamilton-Jacobi-Bellman equation and the other from the stochastic maximum principle. For both formulations, we analyze and compare two numerical methods. The first utilizes the least-squares Monte-Carlo (LSMC) approach for approximating conditional expectations, while the second leverages a time-reversal (TR) of diffusion processes. Although both methods extend to nonlinear settings, our focus is on the linear-quadratic case, where analytical solutions provide a benchmark. Numerical results demonstrate the superior accuracy and efficiency of the TR approach across both BSDE representations, highlighting its potential for broader applications in stochastic control.

## I. INTRODUCTION

Stochastic optimal control (SOC) is central to applications from various disciplines, including finance [1], stochastic thermodynamics [2], [3], robotic navigation [4], [5], and diffusion models [6], [7]. BSDE solutions of stochastic optimal control problem have gained attention in the recent years [8], [9], [10], [11], [12] due to the fundamental challenges of directly solving the Hamilton-Jacobi-Bellman (HJB) partial differential equation (PDE). Namely, there are two BSDEs that arise in the context of stochastic optimal control. The first one is based on the BSDE formulation of the HJB equation, derived from the application of the nonlinear Feynman-Kac lemma [8], [9]. And the second one is obtained from the application of stochastic maximum principle [13]. In the first formulation, the backward process identifies the value function evaluated along the trajectory of the state process. In the second formulation, the backward process is the co-state, which is equal to the derivative of the value function, if the derivative exists, evaluated along the state trajectory. In order to differentiate the BSDEs, the first one is referred to as the value function BSDE, while the second one is referred to as the co-state BSDE.

In both settings, numerical solution of the BSDE is faced with the challenge of finding a forward adapted process that satisfies a terminal constraint. There are several PDE-based approaches [14], [15], [16] that solve the BSDE, but they also suffer from limitations that are similar to solving the HJB equation.

In this paper, we study two sampling-based approaches that numerically approximate the solution to the BSDE.

The first approach is based on expressing the backward process as conditional expectation with respect to the forward filtration [17], [18], [19], [20], [21]. In particular, we focus on [8], [9] where the least-squares Monte-Carlo (LSMC) approach is proposed for numerically approximating the conditional expectations. The second approach is based on time-reversal (TR) of diffusion [22], [23], [24], [25]. Specifically, we study the TR approach, presented as part of our prior work [26], designed to numerically solve the co-state BSDE. The TR formulation reverses the direction of the filtration, thus facilitating the numerical simulation of the backward process, by simply initiating it at terminal time and integrating it backward with the Euler-Maruyama scheme. The TR comes with the additional cost of approximating the so-called Föllmer's drift or score function, for which efficient numerical methods have been developed in the context of diffusion models [27], [28], [29].

The objective of the paper is to study and compare the LSMC and TR approach for solving the value function and co-state BSDEs. In order to do so, we present both algorithms within a unified framework that facilitates the comparison. In doing so, we provide an elementary derivation of the TR formulation for BSDEs, that is more general than the one presented in the prior work, and applies to value function BSDE. We provide extensive numerical results in the linear quadratic (LQ) setting, analyzing the effect of time-discretization, sample size, and problem dimension. Our results demonstrate that solving the co-state BSDE is generally more numerically stable compared to the value function BSDE, and the TR approach gives significantly better accuracy compared to the LSMC. These findings highlight the potential of the TR approach and motivate future research, particularly focusing on the nonlinear setting.

The outline of the paper is as follows: Section II presents the stochastic optimal control problem and the value function and co-state BSDEs. Section III contains the two numerical algorithms, LSMC and TR, that are studied in this paper. Finally, the numerical results and concluding remarks are presented in Section IV and IV, respectively.

## II. PROBLEM FORMULATION AND BACKGROUND

In this paper, we are interested in control systems that are governed by the stochastic differential equation (SDE)

$$dX_t = a(X_t, U_t)dt + \sigma(X_t)dW_t, \quad X_0 \sim p_0, \quad (1)$$

where  $X := (X_t)_{t \geq 0}$  is the  $n$ -dimensional state trajectory,  $U := (U_t)_{t \geq 0}$  is the  $m$ -dimensional control input,  $W := (W_t)_{t \geq 0}$  is the standard  $n$ -dimensional Wiener process, and  $p_0$  is

<sup>1</sup>Y. Mei and A. Taghvaei are with the William E. Boeing department of Aeronautics and Astronautics at University of Washington, Seattle; yuhangm@uw.edu, amirtag@uw.edu. This research is supported by the National Science Foundation (NSF) award EPCN-2347358.

the probability distribution of the initial condition  $X_0$ . The functions  $a: \mathbb{R}^n \times \mathbb{R}^m \rightarrow \mathbb{R}^n$  and  $\sigma: \mathbb{R}^n \rightarrow \mathbb{R}^{n \times n}$  are assumed to be smooth and globally Lipschitz. The control input  $U$  is assumed to be adapted to the filtration  $\mathcal{F}_t = \sigma(W_s; 0 \leq s \leq t)$  generated by the Wiener process  $W$ . This constraint is denoted by  $U_t \in \mathcal{F}_t$  and highlights the non-anticipative nature of the control. The cost function, associated with the control system (1), is

$$J(t, x; U) := \mathbb{E} \left[ \int_t^T \ell(X_s, U_s) ds + \ell_f(X_T) \mid X_t = x \right], \quad (2)$$

for all  $t \in [0, T]$ ,  $x \in \mathbb{R}^n$ , and  $U_t \in \mathcal{F}_t$ , where the running cost  $\ell: \mathbb{R}^n \times \mathbb{R}^m \rightarrow \mathbb{R}$ , and the terminal cost  $\ell_f: \mathbb{R}^n \rightarrow \mathbb{R}$  are assumed to be smooth, and the horizon  $T \in (0, \infty)$  is assumed to be finite. The stochastic optimal problem is to solve the optimization problem

$$\inf_{U_t \in \mathcal{F}_t} \mathbb{E}[J(0, X_0; U)], \quad \text{s.t. (1)}. \quad (3)$$

In the following two subsections, we present two BSDEs that characterize the solution to the SOC problem (3).

#### A. Value function BSDE

The value function is defined according to

$$V(t, x) = \inf_{U_t \in \mathcal{F}_t} J(t, x; U), \quad \forall (t, x) \in [0, T] \times \mathbb{R}^n. \quad (4)$$

The dynamic programming principle implies that the value function solves the HJB PDE [13, Prop. 3.5]

$$\begin{aligned} \partial_t V(t, x) + \inf_u \{ \partial_x V(t, x)^\top a(x, u) + \ell(x, u) \} \\ + \frac{1}{2} \text{Tr}(\partial_{xx} V(t, x) \sigma(x) \sigma(x)^\top) = 0, \quad V(T, x) = \ell_f(x), \end{aligned} \quad (5)$$

for all  $x \in \mathbb{R}^n$  and  $t \in [0, T]$ . Given the value function, the optimal control input is

$$U_t = \arg \min_u \{ \partial_x V(t, X_t)^\top a(X_t, u) + \ell(X_t, u) \} \quad (6)$$

for any realization  $X_t$  of the state process (it is assumed that the minimization (6) has a unique solution).

The HJB equation leads to a BSDE under the following assumption about the model and cost.

*Assumption 1:* The dynamic model admits a control affine form  $a(x, u) = \tilde{a}(x) + \sigma(x) \tilde{B}(x)u$  and the cost function is separable and quadratic in control, i.e.  $\ell(x, u) = \tilde{\ell}(x) + \frac{1}{2}u^\top Ru$  for a positive definite matrix  $R$ .

The BSDE is formally constructed as follows. Let  $X_t$  solve (1) with some control input  $U_t \in \mathcal{F}_t$ . Application of the Itô rule to  $V(t, X_t)$ , along with the HJB equation (5), concludes that

$$\begin{aligned} dV(t, X_t) &= \partial_x V(t, X_t)^\top a(X_t, U_t) dt + \partial_x V(t, X_t)^\top \sigma(X_t) dW_t \\ &- \inf_u \{ \partial_x V(t, X_t)^\top a(X_t, u) + \ell(X_t, u) \} dt, \quad V(T, X_T) = \ell_f(X_T). \end{aligned}$$

Using Assumption 1, and defining the pair

$$(Y_t, Z_t) := (V(t, X_t), \sigma(X_t)^\top \partial_x V(t, X_t)) \quad (7)$$

concludes the BSDE

$$-dY_t = h(X_t, U_t, Y_t, Z_t) dt - Z_t^\top dW_t, \quad Y_T = \ell_f(X_T), \quad (8)$$

where

$$h(x, u, y, z) := \tilde{\ell}(x) - \frac{1}{2} z^\top \tilde{B}(x) R^{-1} \tilde{B}(x)^\top z - z^\top \tilde{B}(x) u, \quad (9)$$

for  $(x, u, y, z) \in \mathbb{R}^n \times \mathbb{R}^m \times \mathbb{R} \times \mathbb{R}^n$ . The optimal control input is identified in terms of the solution with the formula

$$U_t^* = -R^{-1} \tilde{B}(X_t)^\top Z_t. \quad (10)$$

A rigorous analysis of the BSDE (8) and its relation to the nonlinear Feynman-Kac lemma appears in [9].

#### B. Co-state BSDE

The Hamiltonian function for the SOC problem (3) is defined according to

$$H(x, u, y, z) := \ell(x, u) + y^\top a(x, u) + \text{Tr}(z \sigma(x)), \quad (11)$$

for  $(x, u, y, z) \in \mathbb{R}^n \times \mathbb{R}^m \times \mathbb{R}^n \times \mathbb{R}^{n \times n}$ . The Hamiltonian function is used to introduce the BSDE

$$-dY_t = \partial_x H(X_t, U_t, Y_t, Z_t) dt - Z_t^\top dW_t, \quad Y_T = \partial_x \ell_f(X_T), \quad (12)$$

for any control input  $U_t \in \mathcal{F}_t$ , where the pair  $(Y, Z) := (Y_t, Z_t)_{t \geq 0}$  are known as adjoint processes. According to the stochastic maximum principle, the optimal control input  $U_t$  satisfies

$$U_t = \arg \min_u H(X_t, u, Y_t, Z_t), \quad \forall t \in [0, T]. \quad (13)$$

where  $(X, Y, Z)$  are the solutions to (1)-(12) [13, Thm. 3.2, Case 1].

The solution to the BSDE (12) may be expressed in terms of the value function, when it is differentiable, according to

$$(Y_t, Z_t) = (\partial_x V(t, X_t), \sigma(X_t)^\top \partial_{xx} V(t, X_t)). \quad (14)$$

*Remark 1:* The stochastic maximum principle does not require the control-affine model and separable cost Assumption 1.

#### C. Linear quadratic case

A special class of stochastic optimal control problems is the linear quadratic (LQ) case where the dynamic model and cost functions take the special form

$$\begin{aligned} a(x, u) &= Ax + Bu, \quad \sigma(x) = \sigma, \\ \ell(x, u) &= \frac{1}{2} x^\top Qx + \frac{1}{2} u^\top Ru, \quad \ell_f(x) = \frac{1}{2} x^\top Q_f x, \end{aligned}$$

where  $A, B, \sigma, Q, R$ , and  $Q_f$  are matrices of appropriate dimensions. In the LQ case, it is further assumed that  $Q$  and  $Q_f$  are symmetric positive semidefinite matrices, while  $R$  is a symmetric positive definite matrix.

The LQ case is an important benchmark because the exact solution is explicitly known in this case. In particular, the value function  $V(t, x) = \frac{1}{2} x^\top G_t x + g_t$  where  $G_t$  and  $g_t$  solve the differential equations

$$\begin{aligned} -\dot{G}_t &= G_t A + A^\top G_t + Q - G_t B R^{-1} B^\top G_t, \quad G_T = Q_f \\ -\dot{g}_t &= \frac{1}{2} \text{Tr}(\sigma \sigma^\top G_t) \quad g_T = 0 \end{aligned} \quad (15)$$

The optimal control law is given by

$$U_t = -R^{-1}B^\top G_t X_t. \quad (16)$$

The solution to the BSDEs (8) and (12) is also explicitly known and given by

$$\text{BSDE (8): } (Y_t, Z_t) = (\frac{1}{2}X_t^\top G_t X_t, \sigma^\top G_t X_t)$$

$$\text{BSDE (12): } (Y_t, Z_t) = (G_t X_t, \sigma^\top G_t).$$

### III. ALGORITHMS

In this section, we present two algorithms that aim to solve the BSDEs (8) and (12). In both cases, we assume the control input is generated through a feedback control law  $U_t = k(t, X_t)$  for some given function  $k: [0, T] \times \mathbb{R}^n \rightarrow \mathbb{R}^m$ . Later in Section IV, we explain how the solution to the BSDEs is used to iteratively update the feedback control law until convergence to the optimal control law.

In order to facilitate the presentation, the BSDEs (8) and (12) are expressed in the unified form

$$-dY_t = g(t, X_t, Y_t, Z_t)dt - Z_t^\top dW_t, \quad Y_T = g_f(X_T), \quad (17)$$

where, depending on the BSDE,  $g$  and  $g_f$  take the following forms:

$$\text{BSDE (8): } g(t, x, y, z) = h(x, k(t, x), y, z), \quad g_f(x) = \ell_f(x),$$

$$\text{BSDE (12): } g(t, x, y, z) = \partial_x H(x, k(t, x), y, z), \quad g_f(x) = \partial_x \ell_f(x).$$

Furthermore, we assume the PDE

$$\begin{aligned} &\partial_t \phi(t, x) + \partial_x \phi(t, x)^\top a(x, k(t, x)) + \frac{1}{2} \text{tr}(\partial_{xx} \phi(t, x) D(x)) \\ &+ g(t, x, \phi(t, x), \sigma(x)^\top \partial_x \phi(t, x)) = 0, \quad \phi(T, x) = g_f(x), \end{aligned} \quad (18)$$

admits a smooth solution  $\phi$ . Under this assumption, the solution to the BSDE (17) is given by the formula

$$(Y_t, Z_t) = (\phi(t, X_t), \sigma(X_t)^\top \partial_x \phi(t, X_t)). \quad (19)$$

For the case of BSDE (8),  $\phi(t, x) = V(t, x)$  solves the PDE (18), while for BSDE (12),  $\phi(t, x) = \partial_x V(t, x)$  solves the PDE (18), where  $V(t, x)$  is the value function.

The algorithms that are presented below aim at approximating the function  $\phi(t, x)$ , not by solving the PDE (18), but through a sampling-based approach.

#### A. Least-Squares-Monte-Carlo (LSMC)

This section presents the LSMC algorithm, introduced in [8], [9], for approximating the conditional expectation that identifies the solution to the BSDE (17).

Integrating the BSDE over the interval  $[s, t] \subset [0, T]$  and taking the conditional expectation with respect to  $\mathcal{F}_s$  yields

$$Y_s = \mathbb{E}[Y_t + \int_s^t g(\tau, X_\tau, Y_\tau, Z_\tau) d\tau | \mathcal{F}_s].$$

Then, the minimum mean-squared-error property of conditional expectation and the relationship  $Y_s = \phi(s, X_s)$  concludes the following optimization problem for  $\phi(s, \cdot)$

$$\phi(s, \cdot) = \arg \min_{\phi} \mathbb{E}[\|Y_t + \int_s^t g(\tau, X_\tau, Y_\tau, Z_\tau) d\tau - \phi(X_s)\|^2].$$

---

#### Algorithm 1 Least-squares-Monte-Carlo (LSMC)

---

- 1: **Input:** sample size  $N$ , step-size  $\Delta t$ , control law  $k(t, x)$ , function class  $\Phi$ .
  - 2:  $\{X_0^i\}_{i=1}^N \sim p_0$
  - 3: **for**  $t \in \{0, \Delta t, \dots, T - \Delta t\}$  **do**
  - 4:  $U_t^i = k(t, X_t^i)$  and  $\{\Delta W_t^i\}_{i=1}^N \sim N(0, \Delta t I_n)$
  - 5:  $X_{t+\Delta t}^i = X_t^i + a(X_t^i, U_t^i) \Delta t + \sigma(X_t^i) \Delta W_t^i$
  - 6: **end for**
  - 7:  $Y_T^i = g_f(X_T^i)$ ,  $Z_T^i = \sigma(X_T^i)^\top \partial_x g_f(X_T^i)$ , and  $\phi(T, \cdot) = g_f(\cdot)$
  - 8: **for**  $t \in \{T, T - \Delta t, \dots, \Delta t\}$  **do**
  - 9:  $\Delta Y_t^i = g(X_t^i, U_t^i, Y_t^i, Z_t^i) \Delta t$
  - 10:  $\phi(t - \Delta t, \cdot) = \arg \min_{\phi \in \Phi} \sum_{i=1}^N \|Y_t^i + \Delta Y_t^i - \phi(X_{t-\Delta t}^i)\|^2$
  - 11:  $Y_{t-\Delta t}^i = \phi(t - \Delta t, X_{t-\Delta t}^i)$
  - 12:  $Z_{t-\Delta t}^i = \sigma(X_{t-\Delta t}^i)^\top \partial_x \phi(t - \Delta t, X_{t-\Delta t}^i)$
  - 13: **end for**
  - 14: **Output:**  $\{\phi(t, \cdot)\}_{t \in \{0, \Delta t, \dots, T\}}$
- 

Finally, by discretizing the time domain with step-size  $\Delta t > 0$  and generating  $N$  independent realizations of the state trajectory  $\{X_t^i\}_{i=1}^N$ , we end up with a recursive update formula for the function  $\phi$ , such that, given  $\phi(t, \cdot)$ , the function  $\phi(t - \Delta t, \cdot)$  is obtained by solving the minimization problem

$$\phi(t - \Delta t, \cdot) = \arg \min_{\phi \in \Phi} \sum_{i=1}^N \|Y_t^i + g(t, X_t^i, Y_t^i, Z_t^i) \Delta t - \phi(X_{t-\Delta t}^i)\|^2,$$

where  $(Y_t^i, Z_t^i) = (\phi(t, X_t^i), \sigma(X_t^i)^\top \partial_x \phi(t, X_t^i))$ , and  $\Phi$  is a given parametric class of functions. A detailed description of the method is presented in Algorithm 1.

#### B. Time-Reversal (TR)

This section presents a derivation of the TR approach for BSDEs, that is more general and elementary compared to the one introduced in the prior work [26]. In particular, [26] uses the stochastic maximum principle for McKean-Vlasov SDEs to derive the time-reversal formulation of only (12), while, here we use (18) and Itô's formula to derive the time-reversal formulation for both (8) and (12).

The SDE (1), with feedback control  $U_t = k(t, X_t)$ , admits the time-reversal formulation

$$d\tilde{X}_t = a(\tilde{X}_t, k(t, \tilde{X}_t))dt + b(t, \tilde{X}_t)dt + \sigma(\tilde{X}_t) \tilde{d}W_t, \quad \tilde{X}_T \sim p_T \quad (20)$$

where  $\tilde{d}W_t$  denotes backward stochastic integration [30, Sec. 2],  $p_t(x)$  is the probability density function of  $X_t$ ,

$$b(t, x) := -\frac{1}{p_t(x)} \partial_x (D(x)^\top p_t(x))$$

is known as the Föllmer's drift term or score function, and  $D(x) := \sigma(x) \sigma(x)^\top$ . The solution  $\tilde{X}_t$  to the time-reversed SDE (20) is adapted to the backward filtration  $\tilde{\mathcal{F}}_t := \sigma(W_T - W_s; t \leq s \leq T)$ . Moreover, the solution is equal, in probability, to the solution to the SDE (1), i.e. the probability distribution of the path  $\{\tilde{X}_t; 0 \leq t \leq T\}$  is equal to the probability distribution of the path  $\{X_t; 0 \leq t \leq T\}$  [25].

Applying the integration by parts and following [?, Thm. 1], the score function  $b(t, x)$  is the solution to the minimization

$$\min_b \mathbb{E} \left[ \frac{1}{2} \|b(X_t)\|^2 - \text{Tr}(D(X_t) \partial_x b(X_t)) \right].$$

This result is used for the numerical approximation of the score function. In particular, given  $N$  realizations of the state  $\{X_t^i\}_{i=1}^N$ , the score function is approximated by solving the optimization problem

$$\min_{b \in \Psi} \frac{1}{N} \sum_{i=1}^N \left[ \frac{1}{2} \|b(X_t^i)\|^2 + \text{Tr}(D(X_t^i) \partial_x b(X_t^i)) \right], \quad (21)$$

where  $\Psi$  is a given class of functions.

The time-reversed process  $\tilde{X}_t$  is used to construct the time-reversal of the BSDE (17) as follows. Application of the Itô rule to  $\phi(t, \tilde{X}_t)$ , where  $\phi$  is the solution to the PDE (18), concludes

$$\begin{aligned} d\phi(t, \tilde{X}_t) = & -g(t, \tilde{X}_t, \phi(t, \tilde{X}_t), \sigma(\tilde{X}_t)^\top \partial_x \phi(t, \tilde{X}_t)) dt \\ & -c(t, \tilde{X}_t) dt + \partial_x \phi(t, \tilde{X}_t)^\top \sigma(\tilde{X}_t) d\tilde{W}_t, \end{aligned}$$

where  $c(t, x) := \text{Tr}(D(x) \partial_{xx} \phi(t, x)) - \partial_x \phi(t, x)^\top b(t, x)$ . Defining  $(\tilde{Y}, \tilde{Z}) = (\phi(t, \tilde{X}_t), \sigma(\tilde{X}_t)^\top \partial_x \phi(t, \tilde{X}_t))$  concludes the relationship

$$-d\tilde{Y}_t = g(t, \tilde{X}_t, \tilde{Y}_t, \tilde{Z}_t) dt - \tilde{Z}_t^\top d\tilde{W}_t + c(t, \tilde{X}_t) dt, \quad \tilde{Y}_T = g_f(\tilde{X}_T) \quad (22)$$

which is viewed as the time-reversal of the BSDE (17). By construction, the solution  $(\tilde{Y}_t, \tilde{Z}_t)$  is adapted to the backward filtration  $\tilde{\mathcal{F}}_t$ , and the process  $(Y, Z) = \{(Y_t, Z_t); 0 \leq t \leq T\}$  has the same probability law as  $(\tilde{Y}, \tilde{Z}) = \{(\tilde{Y}_t, \tilde{Z}_t); 0 \leq t \leq T\}$ . Moreover, the relationship  $\tilde{Y}_t = \phi(t, \tilde{X}_t)$  implies the following minimization problem to numerically approximate  $\phi(t, x)$ :

$$\min_{\phi \in \Phi} \sum_{i=1}^N \|\tilde{Y}_t^i - \phi(t, \tilde{X}_t^i)\| \quad (23)$$

where  $\{(\tilde{X}_t^i, \tilde{Y}_t^i)\}_{i=1}^N$  are realizations of (20)-(22).

The time-reversed BSDE (22) is used to develop a numerical algorithm to solve BSDEs. Similar to LSMC, the algorithm starts with simulating  $N$  independent realizations of the state process  $\{X_t^i\}_{i=1}^N$  over a discretization of the time-domain. However, the algorithm involves the additional step of approximating the score function by solving the minimization (21). Then, the time-reversed state and adjoint processes (20)-(22) are simulated backward, while simultaneously the minimization problem (23) is solved to obtain the function  $\phi$ . The details are presented in Algorithm 2.

#### IV. NUMERICAL RESULTS

We presented the LSMC and TR algorithms for solving a general BSDE of the form (17). The output of these algorithms is used to compute the optimal control law for the SOC problem (3) according to the following iterative procedure. Starting from an initial feedback control law  $k(t, x)$  (typically chosen to be zero), the algorithms are implemented to obtain the function  $\phi(t, x)$  in the relationship (19). The

#### Algorithm 2 Time-reversal (TR)

---

```

1: Input: sample size  $N$ , step-size  $\Delta t$ , control law  $k(t, x)$ ,
   function class  $\Phi$  and  $\Psi$ .
2:  $\{X_{0:T}^i\}_{i=1}^N \sim p_0$ 
3: for  $t \in \{0, \Delta t, \dots, T - \Delta t\}$  do
4:    $U_t^i = k(t, X_t^i)$  and  $\{\Delta W_t^i\}_{i=1}^N \sim N(0, \Delta t I_n)$ 
5:    $X_{t+\Delta t}^i = X_t^i + a(X_t^i, U_t^i) \Delta t + \sigma(X_t^i) \Delta W_t^i$ 
6:    $b(t, \cdot) = \arg \min_{b \in \Psi} \frac{1}{N} \sum_{i=1}^N [\frac{1}{2} \|b(X_t^i)\|^2 +$ 
      $\text{Tr}(D(X_t^i) \partial_x b(X_t^i))]$ 
7: end for
8:  $\tilde{X}_T^i = X_T^i$ 
9:  $\tilde{Y}_T^i = g_f(\tilde{X}_T^i)$ ,  $\tilde{Z}_T^i = \sigma(\tilde{X}_T^i)^\top \partial_x g_f(\tilde{X}_T^i)$ , and  $\phi(T, \cdot) = g_f(\cdot)$ 

10: for  $t \in \{T, T - \Delta t, \dots, \Delta t\}$  do
11:    $\tilde{U}_t^i = k(t, \tilde{X}_t^i)$  and  $\{\Delta \tilde{W}_t^i\}_{i=1}^N \sim N(0, \Delta t I_n)$ 
12:    $\tilde{X}_{t-\Delta t}^i = \tilde{X}_t^i - a(\tilde{X}_t^i, \tilde{U}_t^i) \Delta t - b(t, \tilde{X}_t^i) \Delta t - \sigma(\tilde{X}_t^i) \Delta \tilde{W}_t^i$ 
13:    $c(t, \tilde{X}_t^i) = \text{Tr}(D(\tilde{X}_t^i) \partial_{xx} \phi(t, \tilde{X}_t^i)) - \partial_x \phi(t, \tilde{X}_t^i)^\top b(t, \tilde{X}_t^i)$ 
14:    $\tilde{Y}_{t-\Delta t}^i = \tilde{Y}_t^i + g(t, \tilde{X}_t^i, \tilde{Y}_t^i, \tilde{Z}_t^i) \Delta t + c(t, \tilde{X}_t^i) \Delta t - (\tilde{Z}_t^i)^\top \Delta \tilde{W}_t^i$ 
15:    $\phi(t - \Delta t, \cdot) = \arg \min_{\phi \in \Phi} \sum_{i=1}^N \|\tilde{Y}_{t-\Delta t}^i - \phi(\tilde{X}_{t-\Delta t}^i)\|^2$ 
16:    $\tilde{Z}_{t-\Delta t}^i = \sigma(\tilde{X}_{t-\Delta t}^i)^\top \partial_x \phi(t - \Delta t, \tilde{X}_{t-\Delta t}^i)$ 
17: end for
18: Output:  $\{\phi(t, \cdot)\}_{t \in \{0, \Delta t, \dots, T\}}$ 

```

---

function  $\phi(t, x)$  is then used to generate the next guess for the optimal control law, depending on which BSDE is solved. In particular,

$$\text{BSDE (8): } k(t, x) = -R^{-1} \tilde{B}(x)^\top \sigma(x)^\top \partial_x \phi(t, x),$$

$$\text{BSDE (12): } k(t, x) = \arg \min_u H(x, u, \phi(t, x), \sigma(x)^\top \partial_x \phi(t, x)).$$

Then, the procedure is iterated until the control law converges.

Given the two BSDEs, (8) and (12), and two different approaches, LSMC and TR, to solve it, we end up with the following four methods to solve the SOC problem:

- LS-V: LSMC method for the value function BSDE (8)
- LS-C: LSMC method for the co-state BSDE (12)
- TR-V: TR method for the value function BSDE (8)
- TR-C: TR method for the co-state BSDE (12)

The algorithms are tested in the LQ setting with the following parametric class of functions, depending on which BSDE is solved:

$$\text{BSDE (8): } \Phi = \{x \mapsto \frac{1}{2} x^\top G x + g; (G, g) \in \mathcal{S}^n \times \mathbb{R}\}$$

$$\text{BSDE (12): } \Phi = \{x \mapsto Gx; G \in \mathbb{R}^{n \times n}\}$$

where  $\mathcal{S}^n$  denotes the space of  $n \times n$  symmetric positive definite matrices. In the LQ setting, the probability distribution of the state  $X_t$  is Gaussian. Consequently, the score function admits the explicit formula

$$b(t, x) = D \Sigma_t^{-1} (X_t - m_t).$$

where  $m_t$  and  $\Sigma_t$  are the mean and covariance matrix for  $X_t$ . The affine form of the score function suggests to choose the

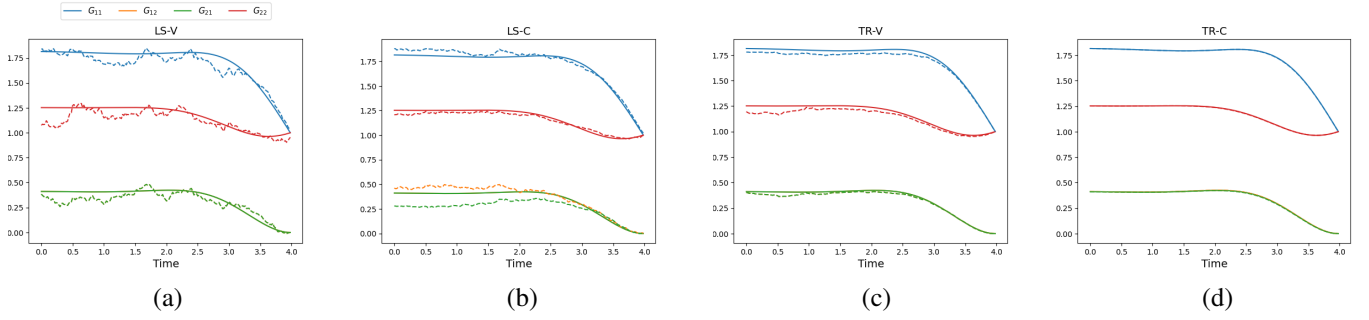


Fig. 1: Numerical result for Section IV-A: The entries of the matrix  $G_t$ , obtained from the four algorithms (a) LSMC-V, (b) LSMC-C, (c) TR-V, and (d) TR-C, in comparison to their exact values. The solid line denotes the exact solution and the dotted line denotes the numerical approximation from algorithms. The time horizon  $T = 4$ , time step-size  $\Delta t = 0.02$ , and sample size  $N = 2000$ .

affine function class

$$\Psi = \{x \mapsto Ax + b; (A, b) \in \mathbb{R}^{n \times n} \times \mathbb{R}^n\}$$

for the score function approximation (21) in the TR algorithm. In fact, in this case, the empirical minimization problem (21) admits an explicit solution  $b(t, x) = D(\Sigma_t^{(N)})^{-1}(X_t - m_t^{(N)})$  where  $m_t^{(N)}$  and  $\Sigma_t^{(N)}$  are the empirical mean and covariance matrix formed from the samples  $\{X_t^i\}_{i=1}^N$ . This formula is used in our numerical implementation of the TR algorithm. The Python code used to generate the results appears in the Github repository<sup>1</sup>.

#### A. Convergence and accuracy

The four algorithms are implemented on a two-dimensional LQ example with the model parameters

$$A = \begin{bmatrix} 0 & 1 \\ -1 & -0.1 \end{bmatrix}, B = \begin{bmatrix} 0 \\ 1 \end{bmatrix}, \sigma = \begin{bmatrix} 1 & 0 \\ 0 & 1 \end{bmatrix}, \\ R = 1, m_0 = \begin{bmatrix} 1 \\ 0 \end{bmatrix}, Q = Q_f = \Sigma_0 = \begin{bmatrix} 1 & 0 \\ 0 & 1 \end{bmatrix}$$

where  $m_0$  and  $\Sigma_0$  are the mean and covariance of the Gaussian initial distribution  $p_0$ . The time horizon  $T = 4$ . The number of samples  $N = 2000$  and the time-discretization step-size  $\Delta t = 0.02$ . All four algorithms start with a zero control law  $k(t, x) = 0$ . Each run of the algorithm results in a  $2 \times 2$  time-varying matrix  $G_t$ , which is used to update the control law according to the formula

$$k(t, x) = -R^{-1}B^\top G_t x.$$

The new control law is used to run the algorithm again, and this procedure is repeated 200 times to ensure convergence and fair comparison among all algorithms.

Figure 1 presents the four entries of the resulting matrix  $G_t$ , after 200 iterations, in comparison to their exact values  $G_t^*$  derived from the Riccati equation (15). The result shows that, although all four algorithms approximate the exact value reasonably, the TR-C algorithm admits much better accuracy compared to the other methods. In order to

quantify this, we introduce the following mean-squared-error (MSE) criteria

$$MSE = \frac{1}{Tn^2} \int_0^T \|G_t^{output} - G_t^*\|_F^2 dt. \quad (24)$$

where  $\|\cdot\|_F$  denotes the Frobenius norm of matrices, and we introduced the factor  $\frac{1}{Tn^2}$  to normalize with respect to the time-horizon and the number of entries in the matrix. The result of approximating the MSE, by averaging over 15 number of simulations and approximating the integral over the discrete-time horizon, appears in Table I, highlighting the significant accuracy of the TR-C method.

Algorithm	MSE
LS-V	$(4.5 \pm 1.9) \times 10^{-3}$
LS-C	$(4.8 \pm 2.5) \times 10^{-3}$
TR-V	$(6.1 \pm 1.5) \times 10^{-4}$
TR-C	$(2.2 \pm 0.4) \times 10^{-6}$

TABLE I: Numerical results for Section IV-A. The MSE (24) evaluated for all four algorithms, averaged over 15 experiments.

The convergence of the SOC cost function through the iterative implementation of the four algorithms is depicted in Figure 2. It is observed that the LS-V and TR-V algorithms both almost converge in one iteration, while the LS-C and TR-C algorithms take longer. This is due to the fact that, solving the value-function BSDE (8) results in the optimal control law (10) irrespective of the control input that is used to generate the state. However, solving the co-state BSDE (12) and updating the control input through (13) results in the optimal control law when the control input that is used to generate the state is itself optimal.

#### B. Effect of time step-size and number of samples

We study the influence of time step size  $\Delta t$  and the number of samples  $N$  on the accuracy of the four methods. In order to do so, we evaluate the MSE (24) averaged over 15 experiments for  $\Delta t \in \{0.004, 0.02, 0.05, 0.1, 0.2, 0.3, 0.4\}$  and  $N \in \{10, 50, 100, 500, 1000, 2000, 4000\}$ . The modelling parameters is identical to the ones selected in Section IV-A.

<sup>1</sup><https://github.com/YuhangMeiUW/LS-TR-BSDE>

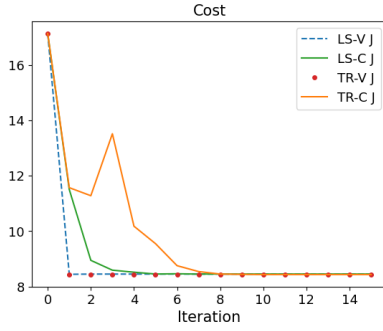


Fig. 2: Numerical result for Section IV-A: The value of the SOC cost (3) in the first 15 iterations of the four methods.

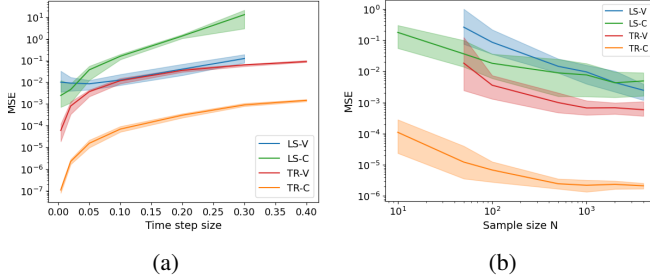


Fig. 3: Numerical results Sec. IV-B. (a) MSE of four methods with  $N = 1000$  and different time step-size  $\Delta t$ ; The experiment is done with time horizon  $T = 4$ , and sample size  $N = 1000$ . (b) MSE of four methods with  $\Delta t = 0.02$  and different number of samples  $N$ . The shaded region represents the range from the minimum to the maximum across 15 experiments.

The result of the experiment with varying time step-size is presented in Figure 3a. It is observed that the MSE of all four methods increases with the time step size, as expected. However, it should be noted that, for the time step  $\Delta t = 0.4$ , the LS-V and LS-C methods experienced numerical instability 7 and 15 times, respectively, out of total 15 experiments. The result shows that the LSMC approach is more sensitive to the step-size.

The result of the experiment with varying number of samples is presented in Figure-3b. It is also observed that the MSE of the four methods decreases as sample size  $N$  increases. And, the LS-V and TR-V algorithm experience numerical instability 11 and 15 times, respectively, out of 15 experiments with a sample size of 10. The result shows the sensitivity of solving value-function BSDE in comparison to co-state BSDE.

The results from both experiments confirm the superior accuracy of the TR-C method, across different time step-size and number of samples.

### C. Scalability with dimension

Our final experiment is concerned with scalability with the problem dimension. In order to do so, we use a mass-spring

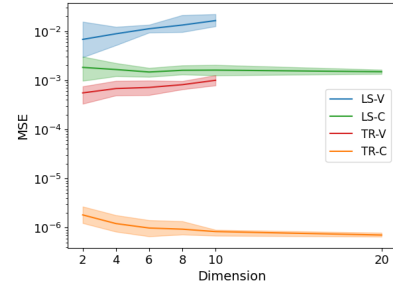


Fig. 4: Numerical results for Section IV-C: MSE of four methods as the problem dimension  $n$  varies. Note that the MSE is normalized by the factor  $n^2$ . The shaded region represents the range from the minimum to the maximum across 15 experiments.

model with the system parameters

$$A = \begin{bmatrix} 0 & I_{p \times p} \\ -\mathbb{T} & -I_{p \times p} \end{bmatrix}, B = \begin{bmatrix} 0 \\ I_{p \times p} \end{bmatrix},$$

$$\Sigma = Q = Q_f = \Sigma_0 = I_{2p \times 2p}, R = I_{p \times p}.$$

where  $p$  is the number of mass-springs in the system,  $\mathbb{T} \in \mathbb{R}^{p \times p}$  is a Toeplitz matrix with 2 on the main diagonal and -1 on the first super and sub-diagonal, and  $I_{p \times p}$  is  $p \times p$  identity matrix. We performed 15 experiments with time step-size  $\Delta t = 0.02$  and fixed sample size  $N = 1000$ , as the dimension  $n = 2p$  varies. The result is depicted in Figure 4. It is observed that the MSE of two TR-C and LS-C methods, that are based on the co-state BSDE, to scale well with the problem dimension. However, the MSE of LS-V and TR-V algorithms increases with the dimension. In fact both approaches experience numerical instability for dimension  $n = 20$ .

## V. CONCLUSIONS

The paper presents a detailed exploration of two different numerical approaches, LSMC and TR, for solving the value function and co-state BSDEs that arise in the context of stochastic optimal control. Through extensive numerical experiments, it was demonstrated that both methods are capable of solving the value function BSDE and the co-state BSDE, with the TR approach outperforming the LSMC method in terms of accuracy and numerical stability, particularly for the co-state BSDE. The results show that the TR method provides superior accuracy, specially in high-dimensional settings and under coarse time discretizations. A possible explanation for this observation is that the denoising procedure in the TR method reduces the noise in the regression problem for solving  $\phi$  compared to the LSMC method. Theoretical justification for this observation is subject of future work. The efficiency of the TR approach, along with its robustness, suggests its potential applicability in a broader range of stochastic control problems beyond the linear-quadratic case, which is the subject of ongoing research.

## REFERENCES

- [1] H. Pham, *Continuous-time stochastic control and optimization with financial applications*. Springer Science & Business Media, 2009, vol. 61.
- [2] K. Sekimoto, *Stochastic energetics*. Springer, 2010, vol. 799.
- [3] L. Peliti and S. Pigolotti, *Stochastic Thermodynamics: An Introduction*. Princeton University Press, 2021.
- [4] S. K. Shah, C. D. Pahlajani, N. A. Lacock, and H. G. Tanner, “Stochastic receding horizon control for robots with probabilistic state constraints,” in *2012 IEEE International Conference on Robotics and Automation*. IEEE, 2012, pp. 2893–2898.
- [5] I. Exarchos, E. A. Theodorou, and P. Tsotras, “Optimal thrust profile for planetary soft landing under stochastic disturbances,” *Journal of Guidance, Control, and Dynamics*, vol. 42, no. 1, pp. 209–216, 2019.
- [6] A. Ramesh, P. Dhariwal, A. Nichol, C. Chu, and M. Chen, “Hierarchical text-conditional image generation with clip latents,” *arXiv preprint arXiv:2204.06125*, vol. 1, no. 2, p. 3, 2022.
- [7] R. Rombach, A. Blattmann, D. Lorenz, P. Esser, and B. Ommer, “High-resolution image synthesis with latent diffusion models,” in *Proceedings of the IEEE/CVF conference on computer vision and pattern recognition*, 2022, pp. 10 684–10 695.
- [8] I. Exarchos and E. A. Theodorou, “Learning optimal control via forward and backward stochastic differential equations,” in *2016 American Control Conference (ACC)*. IEEE, 2016, pp. 2155–2161.
- [9] —, “Stochastic optimal control via forward and backward stochastic differential equations and importance sampling,” *Automatica*, vol. 87, pp. 159–165, 2018.
- [10] M. A. Pereira and Z. Wang, “Learning deep stochastic optimal control policies using forward-backward sdes,” in *Robotics: science and systems*, 2019.
- [11] J. Han, A. Jentzen, and W. E, “Solving high-dimensional partial differential equations using deep learning,” *Proceedings of the National Academy of Sciences*, vol. 115, no. 34, pp. 8505–8510, 2018.
- [12] R. Archibald, “A stochastic gradient descent approach for stochastic optimal control,” *East Asian Journal on Applied Mathematics*, vol. 10, no. 4, 2020.
- [13] J. Yong and X. Y. Zhou, *Stochastic controls: Hamiltonian systems and HJB equations*. Springer Science & Business Media, 1999, vol. 43.
- [14] S. Peng, “Probabilistic interpretation for systems of quasilinear parabolic partial differential equations,” *Stochastics and stochastic reports (Print)*, vol. 37, no. 1-2, pp. 61–74, 1991.
- [15] J. Ma, P. Protter, and J. Yong, “Solving forward-backward stochastic differential equations explicitly—a four step scheme,” *Probability theory and related fields*, vol. 98, no. 3, pp. 339–359, 1994.
- [16] J. Ma, P. Protter, J. San Martín, and S. Torres, “Numerical method for backward stochastic differential equations,” *Annals of Applied Probability*, pp. 302–316, 2002.
- [17] J. Zhang, “A numerical scheme for bsdes,” *The annals of applied probability*, vol. 14, no. 1, pp. 459–488, 2004.
- [18] B. Bouchard and N. Touzi, “Discrete-time approximation and Monte-Carlo simulation of backward stochastic differential equations,” *Stochastic Processes and their applications*, vol. 111, no. 2, pp. 175–206, 2004.
- [19] W. Zhao, L. Chen, and S. Peng, “A new kind of accurate numerical method for backward stochastic differential equations,” *SIAM Journal on Scientific Computing*, vol. 28, no. 4, pp. 1563–1581, 2006.
- [20] C. Bender and R. Denk, “A forward scheme for backward sdes,” *Stochastic processes and their applications*, vol. 117, no. 12, pp. 1793–1812, 2007.
- [21] G. Zhang, M. Gunzburger, and W. Zhao, “A sparse-grid method for multi-dimensional backward stochastic differential equations,” *Journal of Computational Mathematics*, pp. 221–248, 2013.
- [22] B. D. Anderson, “Reverse-time diffusion equation models,” *Stochastic Processes and their Applications*, vol. 12, no. 3, pp. 313–326, 1982.
- [23] U. G. Haussmann and E. Pardoux, “Time reversal of diffusions,” *The Annals of Probability*, pp. 1188–1205, 1986.
- [24] H. Föllmer, “An entropy approach to the time reversal of diffusion processes,” in *Stochastic Differential Systems Filtering and Control: Proceedings of the IFIP-WG 7/1 Working Conference Marseille-Luminy, France, March 12–17, 1984*. Springer, 2005, pp. 156–163.
- [25] P. Cattiaux, G. Conforti, I. Gentil, and C. Léonard, “Time reversal of diffusion processes under a finite entropy condition,” *arXiv preprint arXiv:2104.07708*, 2021.
- [26] A. Taghvaei, “Time-reversal of stochastic maximum principle,” in *IEEE Conference on Decision and Control (CDC)*, 2024.
- [27] Y. Song and S. Ermon, “Generative modeling by estimating gradients of the data distribution,” *Advances in neural information processing systems*, vol. 32, 2019.
- [28] Y. Song, J. Sohl-Dickstein, D. P. Kingma, A. Kumar, S. Ermon, and B. Poole, “Score-based generative modeling through stochastic differential equations,” *arXiv preprint arXiv:2011.13456*, 2020.
- [29] J. Ho, A. Jain, and P. Abbeel, “Denoising diffusion probabilistic models,” *Advances in neural information processing systems*, vol. 33, pp. 6840–6851, 2020.
- [30] E. Pardoux and P. Protter, “A two-sided stochastic integral and its calculus,” *Probability theory and related fields*, vol. 76, no. 1, pp. 15–49, 1987.